Russian Journal of General Chemistry, Vol. 75, No. 5, 2005, pp. 800–806. Translated from Zhurnal Obshchei Khimii, Vol. 75, No. 5, 2005, pp. 847–853.
Original Russian Text Copyright © 2005 by Zaitseva, Zdanovich, Koifman.

Kinetics of Oxidation of “Capped” Zinc Porphyrin Containing a 2,5-Dimethoxyphenylene “Cap” with Organic Peroxides in the Presence of Imidazole

S. V. Zaitseva*, S. A. Zdanovich*, and O. I. Koifman**

* *Institute of Chemistry of Solutions, Russian Academy of Sciences, Ivanovo, Russia*
** *Ivanovo State University of Chemical Engineering, Ivanovo, Russia*

Received August 28, 2003

Abstract—Oxidation of the zinc complex of “capped” 5,15-[2,5-bis(2'-phenyleneoxymethyl)-1,4-dimethoxybenzene]-2,8,12,18-tetramethyl-3,7,13,17-tetrabutylporphyrin with organic peroxides in the presence of imidazole at 298 K results in complete breakdown of the complex. The nitrogen base exerts a significant effect on the rate of metal porphyrin oxidation. The kinetic parameters of the reaction were determined. The structures of the sterically strained metal porphyrin and intermediate products of its oxidation were optimized by PM3 calculations. A geometry analysis shows that the deformations of the macroring increase upon formation of the extra complex and its reaction with peroxides.

It is known that the peroxide oxidation of metal porphyrins and phthalocyanines under aerobic conditions, resulting in their breakdown, is similar to processes leading to the discoloration of chlorophyll and its derivatives. Therefore, the results of physicochemical studies of oxidative degradation of metal porphyrins can be used for simulating the related processes in natural systems [1, 2].

The choice of “capped” porphyrins in which the *meso* positions of the macroring are covalently linked with various bridging groups shielding the reaction center is governed by diversity of their structures and properties. Xylene and toluene are often used as solvents for studying the spectral, coordination, and catalytic properties of porphyrins. However, these solvents can contain appreciable amounts of organic peroxides capable of redox reactions with metal porphyrins (MP) [3–6]. As a part of systematic studies of the behavior of sterically strained zinc porphyrins in reactions with compounds containing available oxygen, we examined in this work the peroxide oxidation of “capped” zinc 5,15-[2,5-bis(2'-phenyleneoxymethyl)-1,4-dimethoxybenzene]-2,8,12,18-tetramethyl-3,7,13,17-tetrabutylporphyrin (ZnP) in the presence of a nitrogen base (imidazole, Im) in *o*-xylene.

The possible oxidation sites in metal porphyrins are both the central atom and the macroring [3–9]. In the case of zinc, apparently, only the second pathway is possible. According to the successively recorded electronic absorption spectra of ZnP and (Im)ZnP in *o*-xylene containing peroxides ($CH_3C_6H_4CH_2OOH$ and $CH_3C_6H_4CH_2OOCH_2C_6H_4CH_3$) (Fig. 1), the chromophore system of the porphyrin is broken down without formation of stable intermediate chromophores. The coordination of the peroxide with the zinc ion is impossible because of the increased basicity of the sterically strained macrocyclic ligand compared to unstrained porphyrins. The enhancement of the base properties of the “capped” zinc porphyrin is also due to the presence of alkyl groups at the β-positions and to the decreased aromaticity of the sterically strained macroring.

Two principally different mechanisms of oxidation of the “capped” zinc porphyrin are possible under the experimental conditions. It is known that hydrogen peroxide can hydroxylate unsaturated organic compounds [8]. Our system contains two diffrentent peroxides ($CH_3C_6H_4CH_2OOH$ and $CH_3C_6H_4CH_2OOCH_2 \cdot C_6H_4CH_3$), and such a reaction can be presented by Scheme 1.

In this case, two π electrons from the macroring pass to the σ levels and become involved in the bonds with two RO groups or with RO and OH groups of the peroxide. As a result, the conjugation in the macroring is broken, and its deformation increases. The resulting compound with the broken conjugation system is unstable and undergoes further transformations with the macroring cleavage. The above step is limiting; the subsequent degradation of the chromophore is, apparently, fast, as no intermediate products were detected in the absorption spectra (Fig. 1a).

Scheme 1.

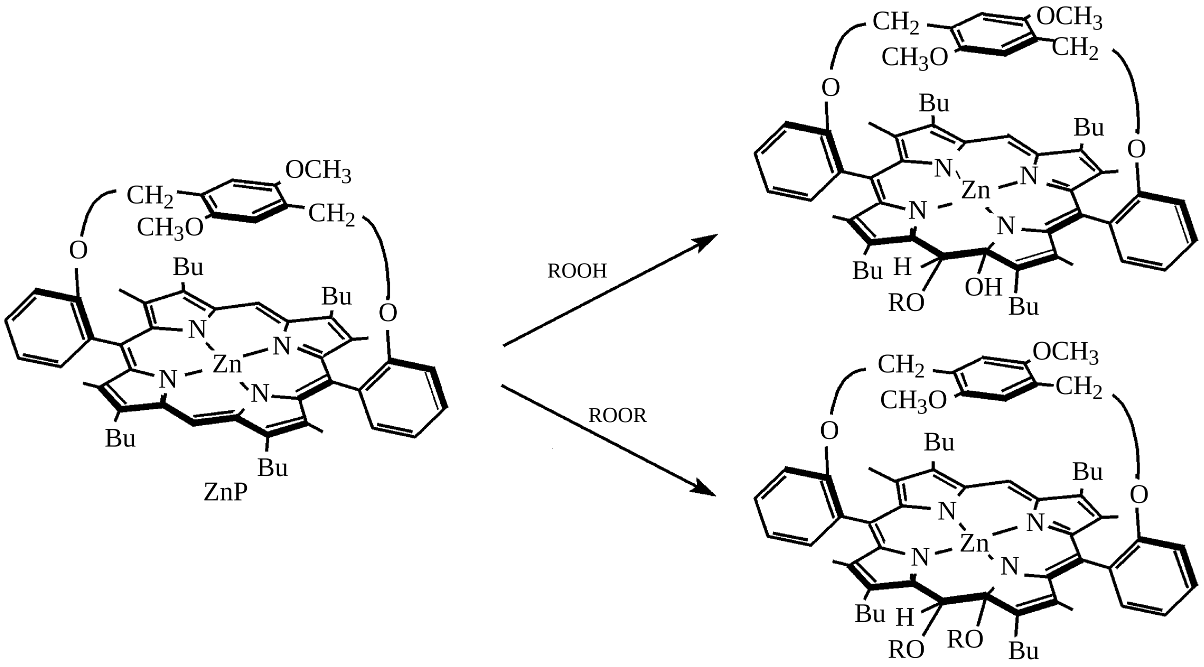

In the presence of imidazole (c_{Im} 10^{-5}–10^{-4} M), the extra complex (Im)ZnP is formed, and it reacts with peroxides along with the initial metal porphyrin.

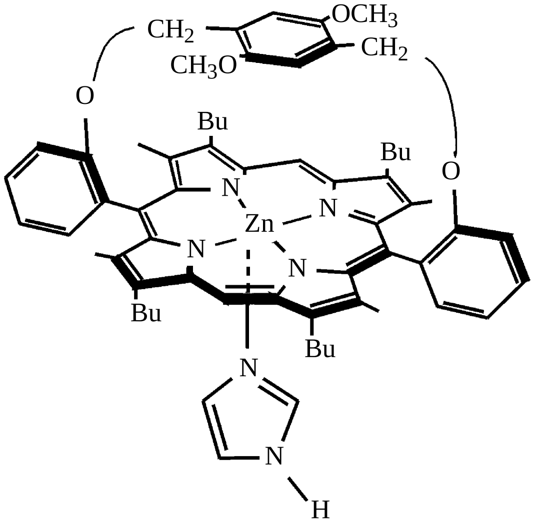

(Im)ZnP

At increased concentrations of imidazole (c_{Im} 10^{-3}–10^{-2} M), the zinc complex completely transforms into the extra complex (Im)ZnP.

Another alternative is the free-radical oxidation mechanism. The radicals $\mathrm{RO}^{\cdot}$ and $\mathrm{HO}^{\cdot}$ generated from peroxides upon their activation react with the sterically strained metal complex at the meso position, giving rise to new radicals $\mathrm{ZnP}^{\cdot}$(RO), $\mathrm{ZnP}^{\cdot}$(HO), and $\mathrm{ZnP}^{\cdot}$ [10].

Presumably, the limiting step in the oxidation of ZnP by this mechanism will be formation of the macrocyclic radical. The arising metal porphyrin radical occurs in the excited state. In this case, it becomes very unstable and immediately undergoes further transformations to give colorless products, which is confirmed by the fact that the spectrum (positions and relative intensities of the main absorption bands) does not change in shape; only the intensities of all the bands decrease proportionally.

As in the oxidation by the first mechanism, the addition of imidazole results in the occurrence of the parallel reactions involving (Im)ZnP instead of ZnP. If the concentration of the base is much higher than that of the metal porphyrin ($c_{\mathrm{Im}} >> c_{\mathrm{ZnP}}$), the only reacting species is the zinc extra complex. In this case, the intermediate species are the macrocyclic radicals (Im)$\mathrm{ZnP}^{\cdot}$(RO), (Im)$\mathrm{ZnP}^{\cdot}$(HO), and (Im)$\mathrm{ZnP}^{\cdot}$.

The optimized structures of the zinc porphyrin molecules also demonstrate the above-noted steric strains in the macroring. According to the results of PM3 calculations, the metal porphyrin in question has a dome-shaped structure (Fig. 2). A specific feature of this compound is that the phenyl substituents together with the methylene bridges of the porphyrin fragment are bent toward the "cap" (the deviation from the mean N_4 plane is 21.12°); as a result, the macroring becomes saddle-shaped (Fig. 2). This structure of this complex is strained and deformed. The coordination of the imidazole molecule gives rise to the *cis* effect

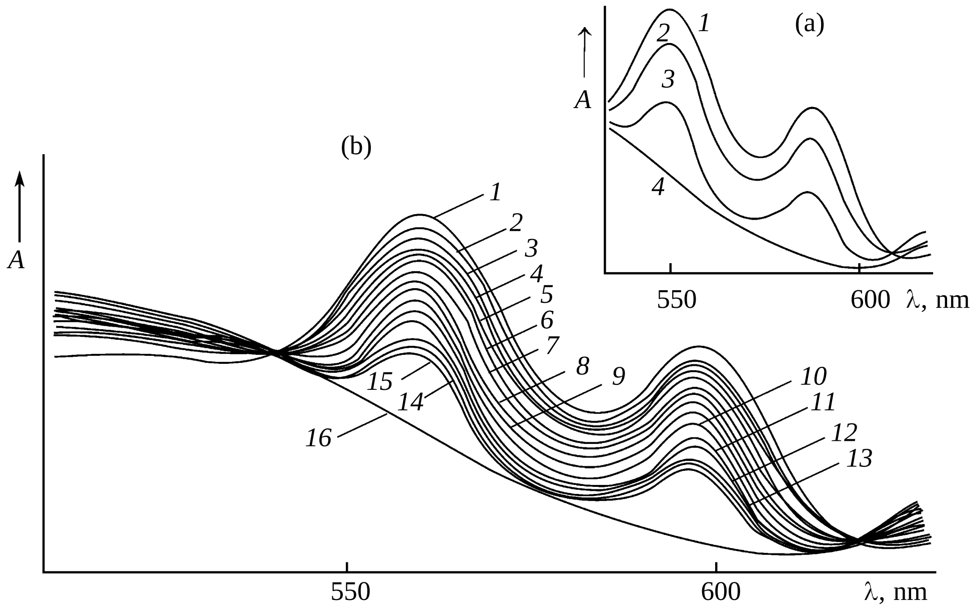

Fig. 1. Electronic absorption spectra. (a) ZnP in *o*-xylene (c_{ZnP} 1.54 × 10^{-5}, c_{perox} 0.9 × 10^{-6} M) at 298 K; τ, s: (*1*) 0, (*4*) 38600, and (*2, 3*) intermediate moments. (b) (Im)ZnP ($c_{(Im)ZnP}$ 1.33 × 10^{-5} M) in *o*-xylene (c_{perox} 0.9 × 10^{-6} M) at 298 K; τ, s: (*1*) 0, (*16*) 17880, and (*2–15*) intermediate moments.

and increases the strain of the porphyrin. According to the calculations, the angle of inclination of the phenyl substituents increases to 25.50°. The formation of the C–OR and C–OH bonds in the complex (Im)ZnP upon oxidation with peroxides is accompanied by further increase in the macroring srtain, manifested in increased deviation of the Zn atom from the coordination plane (Ct–Zn), appreciable decrease in the bond angles in the macroring, and increase in the angle of inclination of the phenyl substituents relative to the N_4 plane (Table 1). As a result, the conjugation is distorted, and the complex is broken down. Thus, presumably, the presence of imidazole accelerates the breakdown of the porphyrin chromophore. This is also indicated by our experimental data (Table 2).

As already noted, the sterically strained “capped” zinc porphyrin, when kept in xylene (c_{perox} in the

Table 1. Geometries of “capped” zinc porphyrin and its derivatives, according to PM3 calculations

Complex	Ct–Zn, Å	$C^1C^{20}C^{19}$, deg	$C^{20}C^{19}C^{18}$, deg	$C^{20}C^{19}C^{24}$, deg	$N^{21}ZnN^{24}$, deg	$N^{21}ZnN^{23}$, deg	$N^{22}ZnN^{24}$, deg	α,[a] deg
ZnP	0.1357	124.49	124.26	126.63	92.39	170.90	172.29	21.12
ZnP(RO)(OH)[b]	0.2069	108.14	117.48	112.38	85.88	168.31	155.07	23.04
ZnP(RO)(OH)[c]	0.4857	118.31	109.24	113.96	88.72	152.49	172.79	24.16
ZnP(RO)(RO)	0.6141	116.57	111.61	115.96	86.35	145.43	162.47	27.30
ZnP(RO)	0.2218	110.02	126.53	125.58	91.02	167.45	172.52	23.16
ZnP(OH)	0.1965	117.85	122.30	127.86	90.13	168.86	174.25	20.75
(Im)ZnP	0.4625	126.23	125.91	125.92	88.23	154.35	154.49	25.05
(Im)ZnP(RO)(OH)[b]	0.6190	108.33	117.88	113.26	83.59	157.09	146.51	24.63
(Im)ZnP(RO)(OH)[c]	0.6267	116.74	112.12	117.29	86.55	145.02	155.23	28.50
(Im)ZnP(RO)(RO)	0.6480	114.67	110.63	115.96	85.70	143.76	155.30	29.00
(Im)ZnP(RO)	0.5429	109.69	123.71	126.11	87.43	150.20	151.51	27.12
(Im)ZnP(OH)	0.5154	117.67	122.08	127.81	87.21	154.53	151.51	24.53

[a] (α) Angle of inclination of the phenyl substituents relative to the N_4 plane. [b] Compound with the OR group at position 20 and OH group at position 19 of the macroring. [c] Compound with the OR group at position 19 and OH group at position 20 of the macroring.

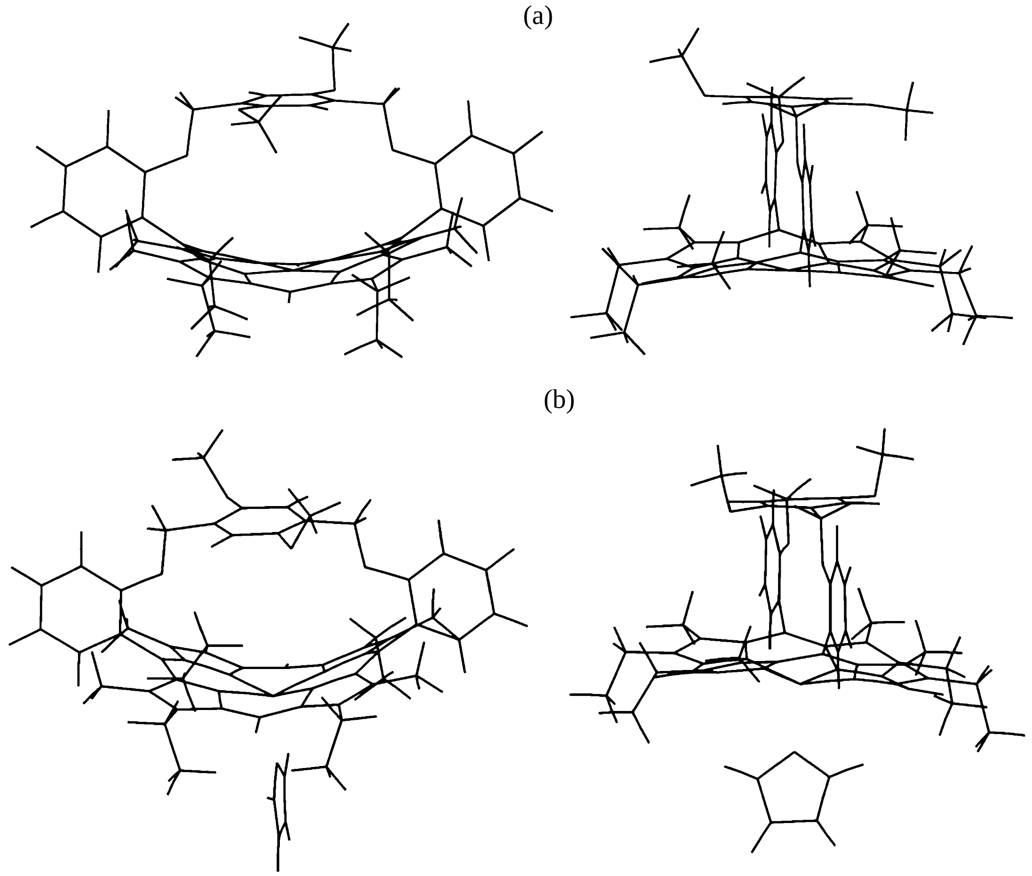

Fig. 2. Structures of (a) ZnP and (b) (Im)ZnP in various projections, according to PM3 calculations.

solvent 0.9×10^{-6} M) in the presence of imidazole at 298 K, is broken down, up to decolorization of the solution (Fig. 1b). In a peroxide-free solution, no oxidation of the metal porphyrin is observed. Let us consider the case when the concentration of the base (1.25×10^{-3} M) is sufficient for instantaneous conversion of the whole amount of ZnP into the extra complex. The order of the breakdown reaction with respect to the peroxide concentration is close to unity, as seen from the approximate constancy (Table 2) of k_{app} of the formally first-order reaction ($n = 1$):

$$dc_{\mathrm{perox}}/d\tau = kc^{n}_{\mathrm{perox}}. \qquad (1)$$

The apparent rate constants k_{app} given in Table 2 were obtained by treatment of the linear dependence $\ln(c/c_0)$–τ [Eq. (2)]:

$$k_{\mathrm{app}} = \frac{1}{\tau}\frac{c_0}{c_\tau}, \qquad (2)$$

where c_0 and c_τ are the peroxide concentrations at times 0 and τ.

The breakdown rate constants k_{app} linearly grow with an increase in the zinc porphyrin concentration (Fig. 3, curve *1*). The rate constants refer to the slow step of the reaction of the peroxide with the complex rather than to the step of the breakdown of the macroring, since at any moment the spectrum (positions and relative intensities of the main absorption bands) of the reaction mixture is similar to the spectrum of the initial extra complex, with only the absolute intensity changing (Fig. 1).

Table 2. Kinetic parameters of the ZnP oxidation with *o*-xylene peroxides (c_{perox} 0.9×10^{-6} M) at 298 K in the presence of imidazole

$c_{\mathrm{Im}} \times 10^3$, M	$c_{\mathrm{ZnP}} \times 10^6$, M	$k_{\mathrm{app}} \times 10^4$, s^{-1}	$c_{\mathrm{Im}} \times 10^3$, M	$c_{\mathrm{ZnP}} \times 10^6$, M	$k_{\mathrm{app}} \times 10^4$, s^{-1}
1.25	1.90	0.492 ± 0.027	0.55	10.6	1.19 ± 0.054
1.25	3.52	0.681 ± 0.024	0.55	17.9	1.68 ± 0.063
1.25	4.82	1.13 ± 0.048	3.07	4.84	0.409 ± 0.038
1.25	13.3	1.98 ± 0.12	3.07	8.90	0.599 ± 0.037
0.55	3.78	0.484 ± 0.034	3.07	9.80	0.640 ± 0.030
0.55	4.61	0.724 ± 0.036	3.07	12.5	0.841 ± 0.029
0.55	8.78	0.929 ± 0.039	3.07	18.0	1.05 ± 0.039

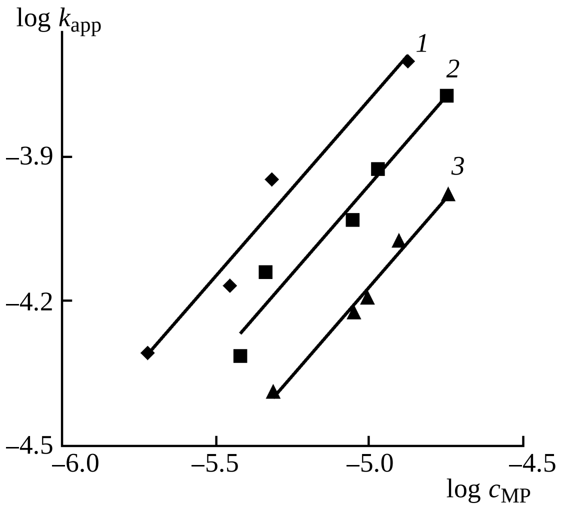

Fig. 3. Plots of $\log k_{app}$ vs. $\log c_{MP}$ at $c_{MP} > c_{perox}$: (*1*) MP = (Im)ZnP, c_{Im} 1.25×10^{-3} M, regression equation $\log k_{app} = 0.74 \log c_{(Im)ZnP} - 0.103$ (*r* 0.96); (*2*) MP = ZnP, c_{Im} 5.5×10^{-4} M, regression equation $\log k_{app} = 0.73 \log c_{ZnP} - 0.296$ (*r* 0.95); (*3*) MP = (Im)ZnP, c_{Im} 3.07×10^{-3} M, regression equation $\log k_{app} = 0.74 \log c_{(Im)ZnP} - 0.495$ (*r* 0.98).

By the least-squares treatment of the experimental data using Eq. (3), we determined the true rate constant (k_v 0.79 s^{-1} mol^{-1} l; for comparison, without imidazole, other conditions being the same, k_v is 0.22 s^{-1} mol^{-1} l) and the reaction order *m* with respect to [(Im)ZnP], which appeared to be equal to 0.74 (i.e., *m* = 1) (Fig. 3, line *1*):

$$\log k_{app} = \log k_v + m \log [(Im)ZnP]. \quad (3)$$

The kinetic equation for the reaction of (Im)ZnP with the peroxide is as follows:

$$-dc_{(Im)ZnP}/d\tau = k_v[(Im)ZnP][Peroxide]. \quad (4)$$

The first orders of the reaction with respect to the metal porphyrin and peroxide indicate that the free radicals $RO^{\cdot}$ and $HO^{\cdot}$ arising in the course of oxidation are deactivated, apparently, on the breakdown products.

It should be noted that, as the imidazole concentration is decreased to 5×10^{-4} M, the apparent rate constants decrease (Table 2). This is due to only partial complexation of ZnP with imidazole, i.e., both (Im)ZnP and ZnP are subject to oxidation:

$$\begin{tikzcd}
ZnP \arrow[r, "k_1"] \arrow[dr, "k_2"'] & (Im)ZnP \arrow[d, "k_3"] \\
& A
\end{tikzcd}$$

Here A are the breakdown products. To construct a general kinetic equation for this case, let us consider each step separately.

$$dc_{(Im)ZnP}/d\tau = k_1[ZnP] - k_3[(Im)ZnP], \quad (5)$$

$$dc_A/d\tau = k_2[ZnP] + k_3[(Im)ZnP], \quad (6)$$

$$-dc_{ZnP}/d\tau = dc_{(Im)ZnP}/d\tau + dc_A/d\tau = k_1[ZnP] - k_3[(Im)ZnP] + k_2[ZnP] + k_3[(Im)ZnP] = [ZnP](k_1 + k_2). \quad (7)$$

As under the conditions of our experiments the extra coordination and peroxide oxidation could not be separated, we determined only the overall rate constant k_v 0.505 s^{-1} mol^{-1} l ($k_v = k_1 + k_2$). The reaction order m with respect to [ZnP] was 0.73 (i.e., *m* = 1) (Fig. 3, line *2*). The order with respect to the peroxide is close to unity, as seen from the satisfactory constancy of k_{app} (Table 2) of the formally first order (*n* = 1). The k_{app} values given in Table 2 were obtained by the treatment of the linear dependence of $\ln(c_0/c_\tau)$ on τ [Eq. (2)].

Taking into account the concentrations of the peroxy compounds, the kinetic equation finally becomes as follows:

$$-dc_{ZnP}/d\tau = k_v[ZnP][Peroxide]. \quad (8)$$

It should be noted that, as the concentration of the base is increased further to 3×10^{-3}–1.6×10^{-2} M, the rate of the peroxide oxidation also decreases (Table 2).

In this case, the kinetic equation has form (4). The reaction orders with respect to the peroxide [Table 2, Eq. (2)] and extra complex (0.74) are close to unity, and the rate constant k_v is 0.32 s^{-1} mol^{-1} l (Fig. 3, line *3*). The constants, as in the above-described cases, refer to the slow step of the reaction of the peroxide with the complex and do not characterize the step of the macroring breakdown.

The inhibiting effect of imidazole at its high concentrations may be due to its capability to bind with peroxides [11] and thus to decrease their activity. Apparently, a large excess of the nitrogen base creates conditions not only for the formation of the extra complex but also for partial binding of peroxy compounds. Thus, the imidazole concentration is one of the factors controlling the oxidation kinetics of the zinc porphyrin.

In all the cases, the first reaction orders with respect to the reactants indicate that the free radicals generated in the course of the oxidation are deactivated on the breakdown products.

Thus, under the examined conditions imidazole activates the peroxide oxidation of the "capped" zinc porphyrin. The facilitated breakdown of the extra complex formed upon adding the base is due to the increased steric strain in the macrocyclic ligand.

EXPERIMENTAL

The electronic absorption spectra were recorded on SF-26 and Specord M-400 spectrophotometers, and the ^{1}H NMR spectra, on a Bruker AC-200 spectrometer (200 MHz, internal reference HMDS, solvent $CDCl_3$).

“**Capped**” **5,15-[2,5-bis(2'-phenyleneoxymethyl)-1,4-dimethoxybenzene]-2,8,12,18-tetramethyl-3,7,-13,17-tetrabutylporphyrin** [12]. A solution of 0.28 g of chloroacetic acid in 30 ml of acetonitrile was added with stirring under nitrogen to a solution of 0.66 g of 3,3'-dibutyl-4,4'-dimethyldipyrrolylmethane and 0.51 g of 2,5-bis(2'-formylphenoxymethyl)-1,4-dimethoxybenzene in 200 ml of acetonitrile. The mixture was stirred in the dark for 4 h, after which 0.85 g of *o*-chloranil in 10 ml of THF was added; the resulting mixture was kept at room temperature for an additional 12 h. The solvent was distilled off, and the residue was washed with an alkali solution and water and dried. After the dissolution in chloroform and double chromatographic purification on alumina in chloroform, the porphyrin was precipitated with methanol and dried. Yield 0.42 g (40%); R_f (Silufol) 0.44 (chloroform). Electronic absorption spectrum, λ_{max}, nm ($\log\varepsilon$): 639 (3.57), 585 (3.84), 551 (3.83), 516 (4.18), 419 (5.32) (chloroform). ^{1}H NMR spectrum, δ, ppm: 9.743 (*meso*-H), 8.929 d, 7.615 m, 7.048 d (PhH), 3.857 m, 2.145 m, 1.744 m, 1.151 t (BuH), 3.476 s (OCH_2), 3.434 s (RH), 2.705 s, 2.548 s (MeH), 1.852 s (OCH_3), –2.553 s (NH).

Zinc complex of “**capped**” **5,15-[2,5-bis(2'-phenyleneoxymethyl)-1,4-dimethoxybenzene]-2,8,-12,18-tetramethyl-3,7,13,17-tetrabutylporphyrin (ZnP)** [13] was prepared by heating the porphyrin with a tenfold excess of zinc acetate in benzene for 2 h. Then the excess salt was washed out with water. The solution was concentrated by vacuum evaporation to a volume of 5–10 ml and chromatographed two times on alumina (Brockmann grade II, eluent benzene). The zinc complex was precipitated with methanol and dried. Yield 95%. Electronic absorption spectrum (*o*-xylene), λ_{max}, nm ($\log\varepsilon$): 587.0 (4.22), 549.0 (4.43), 410.0 (5.34). Found, %: C 74.58; H 7.23; N 5.56. $C_{62}H_{70}N_4O_4Zn$. Calculated, %: C 74.42; H 7.05; N 5.60.

The reaction kinetics was monitored spectrophotometrically [14] at 298 K in *o*-xylene at a working wavelength of 555 nm. The rate constants of the reaction of ZnP with the peroxides were calculated by formally first-order equation (2), with the metal porphyrin being in excess relative to the peroxide.

The quantities k_{app} were optimized and the rms deviations were determined by the least-squares method using the Microsoft Excel programs. The relative error in the determination of k_{app} was 5–10%.

The quantum-chemical calculations were performed in the CNDO approximation [15] by the PM3 method [16–18] with full geometry optimization. The calculation was considered to be complete at a gradient of 0.06 kJ mol^{-1} Å^{-1}.

REFERENCES

1. Konovalova, N.V. and Evstigneeva, R.P., *Usp. Khim.*, 2001, vol. 70, no. 11, p. 1059.
2. Arai, T. and Sato, Y., *Chem. Lett.*, 1990, no. 4, p. 551.
3. Buchler, J.W., Lay, K.L., Caste, L., and Ullrich, V., *Inorg. Chem.*, 1982, vol. 21, no. 2, p. 842.
4. Juan, L.-Ch. and Bruice, T.C., *J. Am. Chem. Soc.*, 1985, vol. 107, no. 2, p. 512.
5. Kropf, H., Spangenberg, J., Gunst, A., and Hinrichsen, J., *Lieb. Ann.*, 1980, no. 12, p. 1923.
6. Dirk, M. and Hambright, P., *J. Chem. Soc., Faraday Trans.*, 1992, vol. 88, no. 14, p. 2013.
7. Liston, D.J. and West, B.O., *Inorg. Chem.*, 1985, vol. 24, no. 10, p. 1568.
8. Berezin, B.D. and Sennikova, G.V., *Kinet. Katal.*, 1968, vol. 9, no. 3, p. 528.
9. Kalish, H., Camp, J.E., Stepien, M., Latos-Grazynski, L., and Balch, A.L., *J. Am. Chem. Soc.*, 2001, vol. 123, no. 47, p. 11719.
10. Bagdasaryan, Kh.S., *Teoriya radikal’noi polimerizatsii* (Theory of Radical Polymerization), Moscow: Nauka, 1966, p. 300.
11. Cheremenskaya, O.V., Solov’eva, F.B., and Ponomarev, G.V., *Zh. Fiz. Khim.*, 2001, vol. 75, no. 1, p. 178.
12. Semeikin, A.S., *Doctoral (Chem.) Dissertation*, Ivanovo, 1995.
13. Zaitseva, S.V., Zdanovich, S.A., Ageeva, T.A., Golubchikov, O.A., and Semeikin, A.S., *Koord. Khim.*, 2001, vol. 27, no. 3, p. 168.
14. *Eksperimental’nye metody khimicheskoi kinetiki*

(Experimental Methods of Chemical Kinetics), Emanuel', N.M. and Sergeev, Eds., G.B., Moscow: Vysshaya Shkola, 1980.

15. Bersuker, I.B., *Elektronnoe stroenie i svoistva koordinatsionnykh soedinenii* (Electronic Structure and Properties of Coordination Compounds), Leningrad: Khimiya, 1986.
16. Schmidt, M.W., Baldridge, K.K., Boatz, J.A., Elbert, S.T., Gordon, M.S., Jensen, J.H., Koseki, S., Matsunaga, N., Nguyen, K.A., Su, S., Windus, T.L., Dupuis, M., and Montgomery, J.A., *J. Comput. Chem.*, 1993, vol. 14, no. 11, p. 1347.
17. Stewart, J.J.P., *J. Computer-Aided Mol. Des.*, 1990, vol. 4, no. 1, p. 1.
18. Fletcher, R., *Methods of Optimization*, New York: Wiley, 1980, p. 45.